Flinders UNIVERSITY

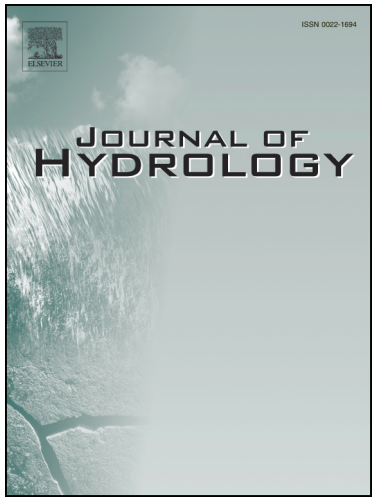

Research papers

Characteristics and causal factors of hysteresis in the hydrodynamics of a large floodplain system: Poyang Lake (China)

X.L. Zhang, Q. Zhang, A.D. Werner, Z.Q. Tan

PII: S0022-1694(17)30561-9
DOI: http://dx.doi.org/10.1016/j.jhydrol.2017.08.027
Reference: HYDROL 22190

To appear in: *Journal of Hydrology*

Received Date: 12 May 2017
Revised Date: 27 July 2017
Accepted Date: 17 August 2017

Please cite this article as: Zhang, X.L., Zhang, Q., Werner, A.D., Tan, Z.Q., Characteristics and causal factors of hysteresis in the hydrodynamics of a large floodplain system: Poyang Lake (China), *Journal of Hydrology* (2017), doi: http://dx.doi.org/10.1016/j.jhydrol.2017.08.027

Characteristics and causal factors of hysteresis in the hydrodynamics of a large floodplain system: Poyang Lake (China)

X. L. Zhang[1, 2], Q. Zhang[1*], A. D. Werner[3], Z. Q. Tan[1]

[1]Key Laboratory of Watershed Geographic Sciences, Nanjing Institute of Geography and Limnology, Chinese Academy of Sciences, Nanjing 210008, China;

[2]University of Chinese Academy of Sciences, Beijing 100049, China;

[3]College of Science and Engineering, and National Centre for Groundwater Research and Training, Flinders University, GPO Box 2100, SA 5001, Australia.

*Corresponding author: Q. Zhang

E-mail address: qzhang@niglas.ac.cn

Tel.: + (86) 025-86882117

Resubmitted to ***Journal of Hydrology*** on July 27th, 2017

Abstract: A previous modeling study of the lake-floodplain system of Poyang Lake (China) revealed complex hysteretic relationships between stage, storage volume and surface area. However, only hypothetical causal factors were presented, and the reasons for the occurrence of both clockwise and counterclockwise hysteretic functions were unclear. The current study aims to address this by exploring further Poyang Lake's hysteretic behavior, including consideration of stage-flow relationships. Remotely sensed imagery is used to validate the water surface areas produced by hydrodynamic modeling. Stage-area relationships obtained using the two methods are in strong agreement. The new results reveal a three-phase hydrological regime in stage-flow relationships, which assists in developing improved physical interpretation of hysteretic stage-area relationships for the lake-floodplain system. For stage-area relationships, clockwise hysteresis is the result of classic floodplain hysteretic processes (e.g., restricted drainage of the floodplain during recession), whereas counterclockwise hysteresis derives from the river hysteresis effect (i.e., caused by backwater effects). The river hysteresis effect is enhanced by the time lag between the peaks of catchment inflow and Yangtze discharge (i.e., the so-called Yangtze River blocking effect). The time lag also leads to clockwise hysteresis in the relationship between Yangtze River discharge and lake stage. Thus, factors leading to hysteresis in other rivers, lakes and floodplains act in combination within Poyang Lake to create spatial variability in hydrological hysteresis. These effects dominate at different times, in different parts of the lake, and during different phases of the lake's water level

fluctuations, creating the unique hysteretic hydrological behavior of Poyang Lake.

Keywords: Lake hydrology; Floodplain; River flow; Hysteresis; Hydrodynamics; Poyang Lake

1. Introduction

Interactions between floodplains, rivers and/or lakes create significant exchanges of water, sediments, nutrients and organic matter, providing fundamental structure and function for wetland plants and aquatic animals (Maltby and Ormerod, 2011; Zedler and Kercher, 2005). In addition to providing unique habitats, particularly for migratory species, floodplains also play an essential role in attenuating flood peaks through the temporary storage of floodwater (Bullock and Acreman, 2003; Hung et al., 2012). The hydrology of floodplains is a function of complex interdependencies between floodplains and adjoining rivers or lakes, involving both surface and subsurface flow pathways (Bates et al., 2000). In some cases, the relationships between different factors pertaining to floodplain hydrological processes have spatial and temporal variations that exhibit some degree of hysteresis (Bates et al., 2000; Hung et al., 2014).

Hysteresis refers to the non-uniqueness of relationships between two variables that arises under cyclic variations (such as seasonal wetting and drying in the case of floodplains), leading to a lag in parameter values depending on the direction of fluctuation (Ewing, 1885). Hysteretic functions have been encountered within a wide range of hydrological processes. These include the moisture retention functions of soils during cyclic wetting and drying (Werner and Lockington, 2006; Zhang et al., 2009), relationships between saturated soil water content and subsurface flow during hillslope runoff events (Norbiato and Borga, 2008), and the stage-discharge rating

curves of rivers (Ajmera and Goyal, 2012; Fread, 2007).

Hysteresis in the hydrological relationships that describe water movement and storage within floodplains arises in a number of forms. For example, Rudorff et al. (2014) found hysteresis in the relationship between flooded area and water level in the large Curuai floodplain, located in the lower reach of the Amazon River. This was attributed to bathymetric features of the Curuai floodplain that direct flood waters to different regions of the floodplain, depending on whether the water level is rising or falling (Rudorff et al., 2014). Hughes (1980) observed hysteresis in the relationship between floodplain inundation volume and the discharge within the neighboring Teifi River (Wales). During recession periods, ponded water remained within the floodplain due to restrictions to drainage, such as slow flows through ebb channels and subsurface pathways. This led to larger inundation volumes during recession relative to periods of flow accession, for a given channel discharge (Hughes, 1980).

Recently, Zhang and Werner (2015) observed hysteretic functions in area-volume-stage relationships for the lake-floodplain system of Poyang Lake (China) based on hydrodynamic modeling. They observed for the first time both clockwise and counterclockwise hysteretic relationships in a single setting. Various modeling scenarios were created to examine the influence of the upstream (i.e., catchment inflows) and downstream (i.e., Yangtze River) boundary conditions, and the role of surface roughness. They concluded that the upstream condition has more influence on the development and magnitude of hysteresis than the downstream condition. In

addition, the degree of hysteresis increased for higher values of surface roughness, particularly in relation to the surface roughness of floodplains rather than regions of permanent inundation. Zhang and Werner's (2015) analysis of hysteresis was based on model simulations (MIKE 21) and has not been substantiated by direct field measurements. What's more, the conditions leading to clockwise and counterclockwise hysteretic relationships have not been established.

This paper aims to extend the knowledge of Poyang Lake hysteretic relationships provided by Zhang and Werner (2015) through the application of remotely sensed imagery and measured data, and by adding catchment inflows and Yangtze River discharge to the list of hydrological parameters that are considered in terms of their hysteretic behavior. It is anticipated that the results of the current study will provide insights into hysteretic processes occurring within other large lake-floodplain settings, such as Lake Tinco (Venezuela; Hamilton and Lewis, 1987), Lake Calado (central Amazon in Brazil; Lesack and Melack, 1995), Lake Tonle Sap (Vietnam; Kummu et al., 2014), and Dongting Lake (China; Chang et al., 2010), where the degree of hysteresis in hydrological relationships has not be determined. The purposes of this research are to: (1) validate Poyang Lake's hysteretic stage-area relationships using remotely sensed imagery; (2) investigate relationships between the flow patterns of the Yangtze River and the Poyang Lake catchment, and lake stage; (3) evaluate the clockwise and counterclockwise hysteresis encountered by Zhang and Werner (2015). The results of this study are expected to provide a more comprehensive understanding

of hysteretic behavior within similar systems comprising extensive floodplains and considerable seasonality in water levels.

2. Description of Study Area

Poyang Lake is located in the middle reach of the Yangtze River (China), within the range 28°24′-29°46′N and 115°49′-116°46′E (Figure 1). The catchment topography varies from mountainous (with maximum elevation of about 2200 m above sea level) to floodplain regions (around 30 m above sea level), covering an area of some 1.62×10^5 km^2 (Zhang et al., 2014). The catchment area of the river gauging stations shown in Figure 1 is 1.37×10^5 km^2, leaving an ungauged area of 0.25×10^5 km^2, which includes the lake surface (Zhang et al., 2014). Land use data from 2005, interpreted from remotely sensed imagery, were categorized into forest (57%), farmland (29%), water bodies (6%), urbanization (6%), pasture (1%) and bare land (1%), with minor changes since 2000 (Li et al., 2014). The catchment has a subtropical wet climate. The mean annual precipitation during 2001-2010 was 1620 mm, calculated from 14 national meteorological stations (Figure 1), with 53% falling between March and June (Figure 2). The mean annual evapotranspiration from the catchment was 780 mm during the period 2001 to 2010, based on the remote sensing investigation by Wu et al. (2013). The mean annual temperature during the same period was 18.1°C, with summer average (June-August) 27.5°C and winter average (December-February) 7.7°C.

[Fig. 1 here]

Fig. 1. Poyang Lake catchment and its location within the Yangtze River Basin.

[Fig. 2 here]

Fig. 2. Intra-annual variation in catchment inflow to Poyang Lake, lake stage measured at Duchang Station, and Poyang Lake catchment precipitation calculated from 14 national meteorological stations, averaged over the period 2001-2010.

Poyang Lake has the most expansive floodplains in China. The extent of flooding varies seasonally under the combined effects of catchment inflow and interactions with the Yangtze River. The lake area varied between 714 and 3163 km^2 during 2001-2010 (Feng et al., 2012). Hydrodynamic models and remote sensing have been applied to study the hydrology of Poyang Lake, and in particular to investigate the seasonal variation in water surface area (Feng et al., 2012; Wu and Liu, 2015a). Previous studies have shown that Poyang Lake has experienced modified conditions in terms of water level and surface area behavior in recent years (e.g., Wu and Liu, 2015a). This has been at least partly attributed to modified interactions between the Yangtze River and Poyang Lake, resulting from the construction and operation of the Three Gorges Dam (Lai et al., 2014; Liu et al., 2016; Zhang et al., 2012).

Poyang Lake receives inflows from five major rivers: the Ganjiang, Xinjiang,

Fuhe, Xiushui and Raohe Rivers, for which gauging data are available from national hydrological stations near their downstream limits (Figure 1). The Lake is connected to the Yangtze River through a relatively narrow channel at its northern extremity. Flows between Poyang Lake and the Yangtze River are monitored at Hukou Station (Figure 1).

Previous attempts to quantify the water balance of Poyang Lake have been made by Zhang et al. (2014). They attributed the outflow at Hukou Station to the summation of gauged runoff, ungauged runoff, groundwater net inflow to the lake and the change in lake volume. In their study, long-term (1953-2010) average outflow at Hukou was 1490×10^8 m^3/y. The average gauged inflow was 1230×10^8 m^3/y. The groundwater inflow was just 1.3% of the water balance and the unknown water balance component, including ungauged runoff and lake volumetric change, was 21% of the inflow. During 2001-2010, the respective proportions of gauged runoff from the Ganjiang, Xinjiang, Fuhe, Xiushui and Raohe Rivers were 57.6%, 14.8%, 9.7%, 9.3% and 8.6%. The average gauged catchment inflow (2001-2010) to Poyang Lake was 1150×10^8 m^3/y. The average inflow from the ungauged catchment area was determined through simple linear extrapolation of the gauged runoff, and equal to 180×10^8 m^3/y. The mean annual precipitation of the lake was about 1650 mm and the potential evaporation was about 1000 mm estimated using the data of nearby meteorological stations (i.e., the Boyang, Lushan and Nanchang Stations; Figure 1) and Penman-Monteith equation (Allen et al., 1998), leading to average net inflow (rainfall

minus evaporation) to the lake surface is relatively small (approximately 13×10^8 m^3/y) based on a mean lake surface area of about 1900 km^2. The average net outflow to the Yangtze River, obtained from gauged records (2001-2010) at Hukou Station, was 1430×10^8 m^3/y. This value accounts for occasional inflows from the Yangtze River (i.e., "backflow"; Li et al., 2017). The difference between average inflows and outflows to Poyang Lake during 2001-2010 is about 270×10^8 m^3/y, or 23% of the total inflow, including groundwater flux into the lake. The above-mentioned estimates of lake water balance components neglect changes in lake storage, because a 10-year average was used and the change in lake storage between the start and end dates was relatively small.

3. Data and Methods

3.1 Hydrological Data

Daily river flow data were obtained for the period 2001-2010, and for the following hydrological monitoring stations: Waizhou (the Ganjiang River), Lijiadu (the Fuhe River), Meigang (the Xinjiang River), Hushan (Le'an tributary of the Raohe River), Dufengkeng (Changjiang tributary of the Raohe River), Wanjiabu (Liaohe tributary of the Xiushui River) and Qiujin (the Xiushui River) (Figure 1). Measurements at Hankou Station represent the discharge of the Yangtze River. The average Yangtze River flow during 2001-2010 was 22,000 m^3/s. The Yangtze River

peaks between July and September. Detailed information about the hydrological stations can be found in Zhang et al. (2014).

The lake water level gauging stations of Kangshan, Tangyin, Duchang, Xingzi and Hukou (from upstream to downstream) were selected to represent the 2001-2010 variations in water levels. Figure 1 illustrates their respective locations. The lake stage measured at Duchang Station varied between 9 and 17 m during 2001-2010 (Figure 2). Kangshan Station, sited near the upstream limit of the lake, reflects more so the conditions near the lake's upstream boundary, whereas Hukou, situated at the junction of the Yangtze River and the lake, displays the influence of the lake's downstream boundary.

3.2 Hydrodynamic Modeling Data

Water surface areas (for the period 2001-2010) were extracted from physically based hydrodynamic modeling of Poyang Lake undertaken by Li et al. (2014), which contains relevant details of the model. Daily time series of water area and stage produced by the model were averaged to monthly time steps using:

$$\overline{H(y,m)} = \frac{1}{n}\sum H(y,t) \quad (1)$$

$$\overline{S(y,m)} = \frac{1}{n}\sum S(y,t) \quad (2)$$

where m and y refers to month (1-12) and year (2001-2010), respectively. H and S are, respectively, stage (m) and water surface area (m^2) on day t ($1 \le t \le 365$) in the

10-year period of analysis, and *n* is the total number of days in month *m* of year *y*, leading to 120 average monthly values of $\overline{H(y,m)}$ and $\overline{S(y,m)}$.

3.3 Remotely Sensed Imagery

Remotely sensed water surface areas of Poyang Lake were derived from 19 scenes of cloud-free Landsat MSS/TM/ETM+ images (at a spatial resolution of 30 m), downloaded from the United States Geological Survey (USGS, 2016). Images were chosen during 2001-2010 to capture both rising and falling periods, ensuring that at least one image was obtained for each one-meter interval in stage change, and so that a reasonably uniform representation of different years and months was obtained (Table 1). Firstly, images were converted to top-of atmosphere (TOA) radiance using radiometric calibration coefficients in the metadata file downloaded from USGS (2016). Then, the calibrated radiance was processed with the FLAASH module embedded in the ENVI 5.1 software (Cooley et al., 2002), resulting in atmospherically corrected surface reflectance (Cui et al., 2011). In this study, the Normalized Difference Water Index (NDWI) (McFeeters, 1996), calculated with green band and near-infrared (NIR) band of geometrically corrected Level 1T (L1T) data, was used to delineate the water surface area. The calculations are described by:

$$NDWI = \frac{DN_{green} - DN_{NIR}}{DN_{green} + DN_{NIR}} \quad (3)$$

where DN_{green} and DN_{NIR} represent the L1T cell values for green and NIR bands,

respectively.

Table 1. Data of selected remotely sensed imagery, corresponding stage measured at Duchang Station, and water surface area interpreted from the selected imagery, which are ordered by the stage.

[Table 1 here]

NDWI is a widely used index in the automated detection of water surfaces (Jain et al., 2005). An optimal NDWI threshold between water surfaces and non-water features was determined using the generated NDWI histogram, and following the technique described by Liu et al. (2012).

3.4 Defining Hysteresis

Stage-flow curves were derived using averaged measured data from 2001-2010, on the basis of the following:

$$\overline{H(t)} = \frac{1}{10}\sum_{y=1}^{10} H(y,t) \quad (4)$$

$$\overline{Q(t)} = \frac{1}{10}\sum_{y=1}^{10} Q(y,t) \quad (5)$$

where H and Q are, respectively, stage (m) and flow (m^3/s) on day t ($1 \le t \le 365$) in the year y (2001-2010) of analysis, resulting in a one-year sequence of average daily

variations $\overline{H(t)}$ and $\overline{Q(t)}$.

To eliminate the dimensional differences, stage, flow and water surface area were normalized in a similar manner to Mishra and Seth (1996), using:

$$\overline{H'(y,m)} = \frac{\overline{H(y,m)} - \overline{H}_{\min}}{\overline{H}_{\max} - \overline{H}_{\min}} \quad (6)$$

$$\overline{S'(y,m)} = \frac{\overline{S(y,m)} - \overline{S}_{\min}}{\overline{S}_{\max} - \overline{S}_{\min}} \quad (7)$$

$$\overline{H'(t)} = \frac{\overline{H(t)} - \overline{H}_{\min}}{\overline{H}_{\max} - \overline{H}_{\min}} \quad (8)$$

$$\overline{Q'(t)} = \frac{\overline{Q(t)} - \overline{Q}_{\min}}{\overline{Q}_{\max} - \overline{Q}_{\min}} \quad (9)$$

where $\overline{H}'$, $\overline{S}'$ and $\overline{Q}'$ are normalized variables. The subscripts 'min' and 'max' are the minimum and maximum values from respective time series of $\overline{H(y,m)}$, $\overline{S(y,m)}$, $\overline{H(t)}$ and $\overline{Q(t)}$. After normalization, the non-dimensional degree of hysteresis (η) was calculated using:

$$\eta_{SH} = \frac{1}{10}\left|\int \overline{S'(y,m)} \cdot d\overline{H'(y,m)}\right| \quad (10)$$

$$\eta_{QH} = \left|\int \overline{Q'(t)} \cdot d\overline{H'(t)}\right| \quad (11)$$

Eqs. (10) and (11) produce an integrated measure of hysteresis that represents the annual summation of hysteretic effects for stage-area curves (η_{SH}) and for stage-flow curves (η_{QH}), in the same manner as Zhang and Werner (2015). Increments in stage, $d\overline{H'(y,m)}$ and $d\overline{H'(t)}$ are positive for rising periods and negative for falling

periods.

4. Results and Discussion

4.1 Stage-Flow Relationships

Figure 3 shows the relationship between average catchment inflow and the lake stage at Duchang Station using time-averaged field measurements (i.e., using Eqs. (4) and (5)). By considering the stage-inflow relationship, we extend the hysteresis analysis of Zhang and Werner (2015). The counterclockwise stage-inflow relationship of Figure 3 indicates that for a given inflow, lake stage is much higher during inflow recession than inflow accession periods, particularly when inflows are low-to-medium.

[Fig. 3 here]

Fig. 3. Relationship between average daily (2001-2010) catchment inflow and lake stage monitored at Duchang. Red symbols represent Phase 1, which is the period between minimum stage (point A) and peak catchment inflow (point B). Green symbols identify Phase 2, which is the period between the peak catchment inflow and peak stage (point C). Blue symbols show Phase 3, which represents the period when stage falls from its maximum to its minimum.

The stage-inflow curve of Figure 3 is characterized by three key events: (1) minimum lake stage (Point A), (2) peak catchment inflow (Point B), and (3) peak lake stage (Point C). As a result, the stage-inflow relationship can be defined according to three phases, as described in the caption of Figure 3. We refer to the duration of each phase as its 'span'. For example, the span of Phase 1 is 171 days. During Phase 1, the catchment inflow rises on average, but exhibits intermittent falls. A key feature of this period is that despite significant variations in catchment inflow, the stage rises with only minor periods of stationarity or gradual decline. The average rate of increase in stage during Phase 1 is 0.035 m/d, and the average rate of increase in catchment inflow is 68 m^3/s/d. There is a sharp increase in catchment inflow immediately prior to Point B (i.e., from 1 June to 20 June), where catchment inflow increases from about 6100 to 12,500 m^3/s, approximately doubling over a period of 20 days. This causes an accompanying stage rise of about 0.87 m over the same period.

The span of Phase 2 is 27 days. In Phase 2, the stage continues to rise as it did in Phase 1, whereas the catchment inflow primarily decreases, with temporary periods of increase. The average rate of stage increase during Phase 2 is 0.030 m/d, which is only slightly less than the corresponding mean value for Phase 1; a surprising result given that the inflow trends in Phases 1 and 2 are opposite in direction. The average decline in catchment inflow in Phase 2 is about 320 m^3/s/d.

The Phase 3 span is 167 days. During Phase 3, the stage drops quickly (0.042 m/d on average), whereas catchment inflow decreases slowly (14 m^3/s/d on average),

including fluctuations between rising and falling. The catchment inflow is almost stable during much of Phase 3, e.g., inflows fell at only 2.5 m^3/s/d from 23 September to 31 October.

A more comprehensive depiction of stage-flow relationships for Poyang Lake is given in Figure 4, which shows one-year time series of daily stage-flow data (i.e., field measurement averages based on Eqs. (4) and (5)) for each river (the Ganjiang, Fuhe, Xinjiang, Raohe, Xiushui and Yangtze Rivers, and total catchment inflow) and gauging station (Hukou, Xingzi, Duchang, Tangyin and Kangshan Stations). These individual depictions of hysteretic relationships between river flow and lake stage allow for a more in-depth interrogation of the spatial variability in hysteretic effects than has been presented in previous hydrological studies of Poyang Lake (Guo et al., 2012; Zhang and Werner, 2015).

[Fig. 4 here]

Fig. 4. Stage-flow relationships given as one-year time series of daily values, which have been averaged over the period 2001-2010. Relationships are shown for the five lake stations and for each river (plus the total catchment inflow). Colors represent the three hydrological phases as described in the caption of Figure 3: Phase 1 (red), Phase 2 (green), and Phase 3 (blue).

Figure 4 shows that stage-flow relationships exhibit counterclockwise hysteresis

between all five catchment rivers (including total catchment inflow) and all five lake stations. Note that Kangshan Station's stage-flow curve has the same hysteretic direction as the other four stations, which differs to the stage-area curves produced by Zhang and Werner (2015). This is discussed in more detail in Section 4.2. The stage-flow relationships between the Yangtze River and lake stations show clockwise hysteresis. The stage-flow functions for catchment rivers have larger loops, i.e., higher degrees of hysteresis, relative to stage-flow curves involving Yangtze River discharge. Trends in hysteresis are shown quantitatively in the Table 2 values of η_{QH}, which were obtained by applying Eqs. (8), (9) and (11) to the data shown in Figure 4.

Table 2. Degree of stage-flow hysteresis (η_{QH}) for each river (and total catchment inflow) and lake station.

[Table 2 here]

Figure 4 and Table 2 show that there is very little hysteresis in stage-flow functions that involve Yangtze River discharge when discharge rates (and water levels) are high. This effect is progressively more dominant for lake stations that are further downstream, and is reflected in smaller values of η_{QH} (involving Yangtze River discharge) for the lake stations closer to the Yangtze River (Table 2). For example, η_{QH} for Kangshan Station is some 14 times larger than that for Hukou Station.

Spatial trends in the degree of hysteresis vary for the five rivers. For example, for

the Ganjiang River, there is an increasing degree of hysteresis from upstream to downstream (i.e., Kangshan to Hukou Stations). However, this trend reverses for the Fuhe River, for which the degree of hysteresis increases in the upstream direction. There are fluctuations in the spatial trends of the degree of hysteresis for other rivers and for the catchment inflow, although the spatial variation in the degree of stage-flow hysteresis is small for the Raohe and Xiushui Rivers. Trends in η_{QH} are at least partly related to the location of the five major rivers that surround the lake (Figure 1) and the uneven inflows from each river. The Raohe and Xiushui Rivers, with small proportions (17.9% in total) of total catchment inflow, have slight effects on lake stage variations, leading to subtle changes in η_{QH}. The Ganjiang and Xinjiang Rivers discharge to the more upstream parts of the lake, and contribute a high proportion (72.4% in total) of catchment inflow, thereby imposing a more dominant influence on the responses of upstream lake stations (i.e., leading to the smaller η_{QH} of Kangshan Station). The same sort of geographical associations are evident in the trends in η_{QH} for rivers that discharge to the central part of the lake (i.e., the Raohe and Xiushui Rivers), which show generally lower hysteresis when compared to centrally located lake stations (e.g., Duchang). Some of the η_{QH} trends in Table 2 are challenging to decipher. For example, the variable pattern of η_{QH} for the Fuhe River may be related to the extensive use of water for irrigation in that region. That is, the largest irrigation scheme of Jiangxi Province is located in the middle and lower reaches of the Fuhe River (Ye et al., 2013). The impact of human activities on local hydrological behavior

is likely to involve complex interrelationships between climate, water use and seasonality, and hence it is difficult to distinguish these in the current analysis.

The span of Phase 2 is shown in Table 3 for each river and lake station. The lake stations that are further upstream produce shorter Phase 2 spans. However, the opposite trend arises from stage-flow relationships involving the Yangtze River, whereby a longer span is obtained for the more upstream lake stations (i.e., from 1 day for Hukou to 27 days for Kangshan; Table 3). This behavior is linked, at least partly, to the position of the lake stations in relation to the two main forces on the lake-catchment inflows and the Yangtze River. For example, lake stations that are further upstream, such as Kangshan and Tangyin, show a more rapid stage response to catchment inflow variations, leading to shorter Phase 2 spans. Thus, the period when river inflows decline and yet stage levels rise is indicative of a wave within the lake, whereby the transition from rising to falling stage progresses from upstream to downstream, with increasing lag relative to the river inflow peak.

Table 3. The span (days) of Phase 2 from stage-flow functions, as derived from the data shown in Figure 4.

[Table 3 here]

Changes at the downstream boundary also create a noticeable wave in the lake, but in this case, the wave propagates upstream. That is, the fall in the Yangtze River

discharge appears to lead to relatively rapid responses at the more downstream lake stations (e.g., Hukou, Xingzi and Duchang Stations), and delayed responses at the more upstream stations (i.e., from 1 day for Hukou to 27 days for Kangshan; Table 3). This reflects the time required for the drop in Yangtze River water levels (i.e., the so-called blocking effect) to traverse the length of Poyang Lake. Thus, stage-flow hysteresis involving the Yangtze River is reversed in direction relative to stage-flow hysteresis involving catchment rivers.

4.2 Stage-Area Relationships

Figure 5 illustrates the relationship between remotely sensed and modeled water surface areas. The scatter points concentrate around the 1:1 line, thereby showing good correlation. This is consistent with the results of model testing by Li et al. (2014), who compared lake areas from the model to 14 remotely sensed images from 2004. They found that dry season lake areas from the model had larger errors (approximately 17%) relative to the model's prediction of wet season lake areas. The larger lake areas calculated by the model may be attributable to several differences between the two methods. For example, in MIKE 21, the lake surface area was determined on the basis of regions where the water depth exceeded a modelling threshold of 10 cm (Li et al., 2014). However, in remotely sensed imagery, the total water surface area depended on the accuracy of NDWI to decipher shallow water areas where the value of NDWI was above 0, which are challenging to resolve where

the water surface is obscured by floodplain vegetation (Liu et al., 2012). The difference between the resolution of Landsat images (i.e., 30 × 30 m), and the size of mesh elements in MIKE 21 (i.e., 70 to 1500 m; Li et al., 2014) may also contribute to discrepancies between the two approaches. In particular, this may partly explain why areas determined using MIKE 21 were larger than those obtained from remotely sensed imagery. Despite methodological differences, the model-remote sensing match is clearly reasonable and serves to validate the simulated model areas produced by Zhang and Werner (2015).

[Fig. 5 here]

Fig. 5. Relationship between water surface areas obtained from remotely sensing and hydrodynamic modeling. The red line represents a perfect match. R^2 is the coefficient of determination, and *p* is the *p*-value (Wilkinson et al., 1973).

The three phases that are apparent in Poyang Lake's stage-flow relationships (Figure 4) are adopted in interpreting stage-area functions, to add to the interpretations of hysteresis provided by Zhang and Werner (2015). The three-phase stage-area curves based on remotely sensed imagery and hydrodynamic modeling are shown in Figures 6(a) and 6(b), respectively. The largest degrees of stage-area hysteresis occur at the more downstream lake stations (e.g., Hukou), and are most evident during low-medium lake stages, as demonstrated by the greater separation

between Phases 1 and 3 in Figure 6. Hysteresis is counterclockwise at these stations. Inter-annual variations produce non-smooth curves, leading to some crossover between rising and falling phases. Nevertheless, the degree of stage-area hysteresis (η_{SH}) shows similar trends with those obtained by Zhang and Werner (2015). That is, except for the clockwise hysteresis of Kangshan Station, the degree of hysteresis reduces in the upstream direction for stations showing counterclockwise hysteresis (Table 4). The stage-area curve of Tangyin Station, located closest to the center of the lake, exhibits the smallest hysteresis effect.

[Fig. 6 here]

Fig. 6. Three-phase stage-area curves of (a) remotely sensed imagery, and (b) hydrodynamic modeling using Eqs. (1) and (2). Stage data are from the five lake stations. Colors represent the three hydrological phases as described in the caption of Figure 3: Phase 1 (red), Phase 2 (green), and Phase 3 (blue).

Table 4. Degree of stage-area hysteresis (η_{SH}) for each lake station using Eq. (10) applied to normalized area and stage datasets obtained by applying Eqs. (6) and (7). Values are derived from the data shown in Figure 6(b).

[Table 4 here]

Zhang and Werner (2015) hypothesized that the time lag between the draining of

the floodplain and the drop in lake stage causes larger floodplain areas during recession relative to accession periods. Zhang and Werner (2015) attribute the counterclockwise hysteresis of Kangshan Station to this process.

Clockwise hysteresis and the greater degree of stage-area hysteresis for downstream lake stations is linked to Poyang Lake's water fluctuation paradigm. That is, Wu and Liu (2015b) showed that lake stage increases from north to south (i.e., from downstream to upstream) during rising periods and decreases from south to north during falling periods based on remotely sensed imagery, which is in accordance with the variations of Phase 2 span (Table 3). That is, for catchment inflow, more downstream (i.e., northern) lake stations (e.g., Hukou Station) have a longer Phase 2 span than upstream (i.e., southern) lake stations (e.g., Kangshan Station) (Table 3).

Figure 6 also shows that when the lake stage is higher than about 16 m, all stations exhibit reduced stage-area hysteresis. That is, lake areas expand and contract in direct response to the rise and fall in lake stage, as expected for a typical lake setting (e.g., Adams and Stoker, 1985) where the hysteretic effects normally associated with rivers (e.g., Ajmera and Goyal, 2012) and floodplains (e.g., Rudorff et al., 2014) are absent. Thus, the system acts more so as a lake when water levels are high. This observation builds on Zhang and Werner's (2015) characterization of Poyang Lake's hysteretic behavior. The spatiotemporal trends in water levels, and their links to Poyang Lake's hysteretic relationships, are further explored in the following sub-section.

4.3 Spatiotemporal Water Level Behavior

Figure 7 presents one-year sequences of average stage variations at the five lake stations, and the accompanying flow hydrographs for the Yangtze River discharge and the total catchment inflow. The discharge of the Yangtze River (at Hankou Station) peaks 1-2 months later than Poyang Lake's catchment inflow. The gray shaded area shows the time lag between the peaks in Yangtze discharge and catchment inflow.

[Fig. 7 here]

Fig. 7. Average daily datasets of (a) stage variations at the five lake stations, and (b) flow hydrographs for the Yangtze River and the Poyang Lake catchment. The gray area highlights the time lag between the peaks of Yangtze River discharge and catchment inflow.

The stage variations depicted in Figure 7 show the periods when two or more lake stations have corresponding water levels, i.e., indicating that the lake water surface of at least part of the lake is flat. The lake is downstream-controlled under these conditions. This is apparent at all of the gauging stations for about 100 days (from 19 June to 27 September; Figure 7), covering the period of highest water levels. The three most downstream lake stations (Duchang, Xingzi and Hukou) continue to have consistent water levels for another 30 days thereafter (i.e., from 27 September to 27

October). Otherwise, an upstream-to-downstream water level gradient is apparent between the lake stations. That is, downstream controls on water levels are only apparent during high water levels and the early stages of recession, whereas a strong spatial water level gradient remains during the majority of rising water level periods. The spatial gradient in lake water levels is flatter during the recession period (Phase 3), and therefore, the water-level decline at downstream lake stations is more closely linked to upstream water-level decline. The lake is relatively narrow in the region north of Duchang (see Figure 1), and therefore, upstream water level decline is the primary driver of reductions in the lake surface area. Hence, compared to the rising period, the lake surface area is smaller during recession periods (for a given water level at downstream stations), giving rise to the counterclockwise hysteresis that is apparent in Figure 6. This adds to Zhang and Werner's (2015) explanation of Poyang Lake's area-stage hysteresis, and arises by combining the three stage-flow phases (Section 4.1) with the stage-area hysteresis described in this section.

The hysteretic stage-area behavior of downstream lake stations (i.e., apparent in Figure 6) is, at least in part, influenced by the lake's shape. As discussed above, the upstream half of lake primarily dictates the trends in the lake surface area. Consequently, the water level trends at the upstream lake stations, rather than those of downstream lake stations, correlate more so to lake area trends. This is reflected in the small hysteresis in stage-area functions of Duchang, Tangyin and Kangshan Stations (Figure 6). Zhang and Werner (2015) also considered the shape of the lake in

providing interpretations of the hysteresis causal factors. They suggested that the wider floodplain areas of more upstream parts of the lake cause a closer association of total lake area with changes in stage in the upstream part of the lake. This causes the stages at upstream stations (e.g., Kangshan Station) to respond commensurately with changes in floodplain areas and catchment inflow. Downstream regions show significant time lag in stage-area functions, because of the time required for the flood wave to traverse the lake's considerable length. This creates the larger hysteresis in hydrological functions of downstream stations, given the association between the span of Phase 2 (i.e., representing the time lag between peak flow and peak stage) and the degree of hysteresis. That is, more downstream lake stations (e.g., Hukou Station) have a longer Phase 2 span (Table 3) and larger η_{SH} (Table 4) than upstream lake stations (e.g., Kangshan Station). Superimposed on this effect is the more rapid response of downstream stations to backwater effects, as demonstrated by smaller Phase 2 spans of downstream stations (e.g., Hukou Station) when related to Yangtze River discharge. The two mechanisms are additive and create the complex hysteretic functions (i.e., both clockwise and counterclockwise directions) of Poyang Lake.

The catchment inflow-Yangtze River time lag shown in Figure 7 plays a critical role in the development of hysteresis. For example, during a 37-day period (20 June to 27 July; gray shaded area in Figure 7), catchment inflow declines rapidly, whereas Yangtze discharge steadily rises. The recession in catchment inflow is more gradual once the Yangtze River peak has passed. Before the peak catchment inflow, lake water

storage and stage rise quickly, driving strong outflows from Poyang Lake to the Yangtze River and creating a massive lake force (Guo et al., 2012). After the peak of catchment inflow, the so-called 'blocking effect' of the Yangtze River creates a downstream control on lake water levels, as discussed in numerous previous publications (Hu et al., 2007; Zhang et al., 2012). Thus, the catchment inflow-Yangtze discharge time lag results in considerably higher lake stage during catchment inflow recession relative to the period of accession, for a given catchment inflow. This creates the counterclockwise hysteresis evident in Figure 4, and is consistent with hysteretic effects observed in rivers caused by downstream controls during recession periods (e.g., Mander, 1978). This explanation of the importance of the time lag between the peaks of Yangtze discharge and catchment inflow (Figure 7) in the development of stage-flow hysteresis (see Figure 4) extends Zhang and Werner's (2015) analysis.

The clockwise hysteresis in stage-flow relationships (Figure 4) involving Yangtze River discharge also arises as a consequence of the catchment inflow-Yangtze discharge time lag. That is, the Yangtze River is largely unresponsive during catchment inflow accession (Phase 1), which causes the lake stage to rise, particularly at the more upstream lake stations. However, catchment inflow declines well before the Yangtze River discharge reduces, and therefore, the lake stage is significantly lower during recession periods (Phase 3) for a given Yangtze River discharge. The result of this is clockwise hysteresis in the Yangtze River stage-flow curves of Figure

4.

5. Conclusions

This research has added further explanation of the significant hysteresis in Poyang Lake's hydrological functions. Additionally, we extend the characterization of Poyang Lake hysteresis by including remotely sensed imagery and relationships between river discharge and lake stage. Remotely sensed imagery serves to validate previous hydrodynamic modeling results, while stage-flow functions identify strong hysteretic relationships. Stage-flow relationships show counterclockwise hysteresis when catchment river inflow is considered, whereas clockwise hysteresis is observed when stage-flow functions involve Yangtze River discharge.

Poyang Lake's stage-area functions show both clockwise and counterclockwise hysteresis, as noted in a previous investigation. We attribute this duality in hysteretic direction to the bimodal river-floodplain characteristics of Poyang Lake. That is, counterclockwise hysteresis in stage-area functions is similar to that observed previously in the behavior of river systems, whereas clockwise hysteresis in stage-area functions is similar to that observed in prior studies of floodplain systems. Added to this, stage-area functions lack hysteresis when the stage exceeds 16 m, thereby resembling the hydrology of a lake system. Thus, the lake stage-area hysteresis of Poyang Lake is in fact tri-modal, representing three different hydrological settings: lake, river and floodplain. The major hysteresis control is the

river effect, which is driven by the time lag between peaks of catchment inflows and Yangtze River discharge. The river effect also causes a significant time lag between peak flow and peak stage, whereby the lake stage continues to rise despite rapid declines in the catchment inflow. This leads to different hysteretic directions in the catchment stage-inflow and Yangtze stage-discharge functions.

By considering Poyang Lake's hydrological functions as the summation of three different hydrological systems (lake, river and floodplain), we are able to identify the role of each in influencing Poyang Lake's hydrology. The three sources of control on Poyang Lake's hydrology each dominate at different times, in different parts of the lake, and during different phases of the lake's water level fluctuations. This adds to the current perception of the hydrology of lakes, which exhibit hysteretic behavior once floodplain inundation or downstream effects occur.

Future investigations of Poyang Lake's hydrology should consider the individual controlling factors of all three elements, and the manner in which they act in combination to produce the complex spatiotemporal water-level variations and stage-flow-area relationships of Poyang Lake. Furthermore, the hysteretic effects of floodplain vegetation and the associated seasonal inundation, in addition to the interrelationship between the lake and surrounding aquifers, should be further investigated given difficulties in simulating these effects in previous hydrodynamic models.

Acknowledgements:

The data presented in this article were provided and quality-controlled by the Changjiang Water Resources Commission (China). This work is supported by the National Science Foundation of China (41371062) and the Collaborative Innovation Center for Major Ecological Security Issue of Jiangxi Province and Monitoring Implementation (JXS-EW-00). Adrian Werner is supported by the Australian Research Council's Future Fellowship scheme (project number FT150100403). Zhiqiang Tan is supported by the Science Foundation of Nanjing Institute of Geography and Limnology, Chinese Academy of Sciences (NIGLAS2017QD05). Jing Yao maintained the hydrodynamic model of Poyang Lake. We thank two anonymous peer reviewers for their constructive comments that assisted in improving this article.

References

Adams, D.B., Stoker, Y.E., 1985. Hydrology of Lake Placid and adjacent area, Highlands County, Florida. U.S. Geological Survey Water-Resources Investigations Report 84-4149, 1 sheet.

Ajmera, T.K., Goyal, M.K., 2012. Development of stage-discharge rating curve using model tree and neural networks: An application to Peachtree Creek in Atlanta. Expert Systems with Applications, 39(5): 5702-5710. DOI: 10.1016/j.eswa.2011.11.101.

Allen, R.G., Pereira L.S., Raes, D., Smith, M., 1998. Crop evapotranspiration - Guidelines for computing crop water requirements, FAO irrigation and drainage paper 56. Food and Agriculture Organization of the United Nations, Rome, Italy.

Bates, P.D., Stewart, M.D., Desitter, A., Anderson, M.G., Renaud, J.P., Smith, J.A., 2000. Numerical simulation of floodplain hydrology. Water Resources Research, 36(9): 2517-2529. DOI: 10.1029/2000WR900102.

Bullock, A., Acreman, M., 2003. The role of wetlands in the hydrological cycle. Hydrology and Earth System Sciences, 7(3): 358-389. DOI: 10.5194/hess-7-358-2003.

Chang, J., Li, J., Lu, D., Zhu, X., Lu, C., Zhou, Y., Deng, C., 2010. The hydrological effect between Jingjiang River and Dongting Lake during the initial period of Three Gorges Project operation. Journal of Geographical Sciences, 20(5):

771-786. DOI: 10.1007/s11442-010-0810-9.

Cooley, T., Anderson, G.P., Felde, G.W., Hoke, M.L., 2002. FLAASH, a MODTRAN4-based atmospheric correction algorithm, its application and validation. Geoscience and Remote Sensing Symposium. IGARSS '02. 2002 IEEE International, Vol. 3, pp. 1414-1418. DOI: 10.1109/IGARSS.2002.1026134.

Cui, B.L., Li, X.Y., Li, Y.T., Ma, Y.J., Yi, W.J., 2011. Runoff characteristics and hysteresis to precipitation in the Qinghai Lake Basin: A case study of Buha river basin. Journal of Desert Research, 31(1): 247-253. (in Chinese with English abstract)

Ewing, J.A., 1885. Experimental researches in magnetism. Philosophical Transactions of the Royal Society of London, 176: 523-640. DOI: 10.1098/rstl.1885.0010.

Feng, L., Hu, C., Chen, X., Cai, X., Tian, L., Gan, W., 2012. Assessment of inundation changes of Poyang Lake using MODIS observations between 2000 and 2010. Remote Sensing of Environment, 121(2): 80-92. DOI: 10.1016/j.rse.2012.01.014.

Fread, D.L., 2007. Computation of stage-discharge relationships affected by unsteady flow. Journal of the American Water Resources Association, 11(2): 213-228. DOI: 10.1111/j.1752-1688.1975.tb00674.x.

Guo, H., Hu, Q., Zhang, Q., Feng, S., 2012. Effects of the Three Gorges Dam on Yangtze River flow and river interaction with Poyang Lake, China. Journal of

Hydrology, 416-417: 19-27. DOI: 10.1016/j.jhydrol.2011.11.027.

Hamilton, S.K., Lewis, W.M., 1987. Causes of seasonality in the chemistry of a lake on the Orinoco River floodplain, Venezuela. Limnology and Oceanography, 32(6): 1277-1290. DOI: 104319/lo.1987.32.6.1277.

Hu, Q., Feng, S., Guo, H., Chen, G., Jiang, T., 2007. Interactions of the Yangtze River flow and hydrologic processes of the Poyang Lake, China. Journal of Hydrology, 347(1-2): 90-100. DOI: 10.1016/j.jhydrol.2007.09.005.

Hughes, D.A., 1980. Floodplain inundation: Processes and relationships with channel discharge. Earth Surface Processes, 5(3): 297-304. DOI: 10.1002/esp.3760050308.

Hung, N.N., Delgado, J.M., Güntner, A., Merz, B., Bárdossy, A., Apel, H., 2014. Sedimentation in the floodplains of the Mekong Delta, Vietnam. Part I: suspended sediment dynamics. Hydrological Processes, 28(7): 3132–3144. DOI: 10.1002/hyp.9856.

Hung, N.N., Delgado, J.M., Tri, V.K., Hung, L.M., Merz, B., Bárdossy, A., Apel, H., 2012. Floodplain hydrology of the Mekong Delta, Vietnam. Hydrological Processes, 26(5): 674-686. DOI: 10.1002/hyp.8183.

Jain, S.K., Singh, R.D., Jain, M.K., Lohani, A.K., 2005. Delineation of flood-prone areas using remote sensing techniques. Water Resources Management, 19(4): 333-347. DOI: 10.1007/s11269-005-3281-5.

Kummu, M., Tes, S., Yin, S., Adamson, P., Józsa, J., Koponen, J., Richey, J., Sarkkula,

J., 2014. Water balance analysis for the Tonle Sap Lake-floodplain system. Hydrological Processes, 28(4): 1722-1733. DOI: 10.1002/hyp.9718.

Lai, X.J., Jiang, J., Yang, G.S., Lu, X.X., 2014. Should the Three Gorges Dam be blamed for the extremely low water levels in the middle–lower Yangtze River? Hydrological Processes, 28(1): 150-160. DOI: 10.1002/hyp.10077.

Lesack, L.F.W., Melack, J., 1995. Flooding hydrology and mixture dynamics of lake water derived from multiple sources in an Amazon floodplain lake. Water Resources Research, 31(2): 329–346. DOI: 10.1029/94WR02271.

Li, Y., Zhang, Q., Werner, A.D., Yao, J., Ye, X., 2017. The influence of river-to-lake backflow on the hydrodynamics of a large floodplain lake system (Poyang Lake, China). Hydrological Processes, 31(1): 117-132. DOI: 10.1002/hyp.10979.

Li, Y., Zhang, Q., Yao, J., Werner, A.D., Li, X., 2014. Hydrodynamic and hydrological modeling of the Poyang Lake catchment system in China. Journal of Hydrologic Engineering, 19(3): 607-616. DOI: 10.1061/(ASCE)HE.1943-5584.0000835.

Liu, Y., Song, P., Peng, J., Ye, C., 2012. A physical explanation of the variation in threshold for delineating terrestrial water surfaces from multi-temporal images: Effects of radiometric correction. International Journal of Remote Sensing, 33(18): 5862-5875. DOI: 10.1080/01431161.2012.675452.

Liu, Y., Wu, G., Guo, R., Wan, R., 2016. Changing landscapes by damming: the Three

Gorges Dam causes downstream lake shrinkage and severe droughts. Landscape Ecology, 31(8): 1883-1890. DOI: 10.1007/s10980-016-0391-9.

Maltby, E., Ormerod, S., 2011. Freshwaters - Openwaters, wetlands and floodplains. In: The UK National Ecosystem Assessment: Technical Report (first edn). UNEP-WCMC, Cambridge, pp. 295-360.

Mander, R.J., 1978. Aspects of unsteady flow and variable backwater. In: Herschy, R.W. (Ed.), Hydrometry: Principles and Practice (first edn). John Wiley & Sons, Chichester.

McFeeters, S.K., 1996. The use of Normalized Difference Water Index (NDWI) in the delineation of open water features. International Journal of Remote Sensing, 17(7): 1425-1432. DOI: 10.1080/01431169608948714.

Mishra, S.K., Seth, S.M., 1996. Use of hysteresis for defining the nature of flood wave propagation in natural channels. Hydrological Sciences Journal, 41(2): 153-170. DOI: 10.1080/02626669609491489.

Norbiato, D., Borga, M., 2008. Analysis of hysteretic behaviour of a hillslope-storage kinematic wave model for subsurface flow. Advances in Water Resources, 31(1): 118-131. DOI: 10.1016/j.advwaters.2007.07.001.

Rudorff, C.M., Melack, J.M., Bates, P.D., 2014. Flooding dynamics on the lower Amazon floodplain: 1. Hydraulic controls on water elevation, inundation extent, and river- floodplain discharge. Water Resources Research, 50(1): 619-634. DOI: 10.1002/2013WR014091.

USGS (2016). United States Geological Survey. USGS Global Visualization Viewer. (Available at http://glovis.usgs.gov, last accessed 9 Dec 2016).

Werner, A.D., Lockington, D.A., 2006. Artificial pumping errors in the Kool–Parker scaling model of soil moisture hysteresis. Journal of Hydrology, 325(1): 118-133. DOI: 10.1016/j.jhydrol.2005.10.012.

Wilkinson, G.N., Rogers, C.E., 1973. Symbolic descriptions of factorial models for analysis of variance. Journal of the Royal Statistical Society, 22(3), 392–399. DOI: 10.2307/2346786.

Wu, G.P., Liu, Y.B., Zhao, X.S., Ye, C., 2013. Spatio-temporal variations of evapotranspiration in Poyang Lake Basin using MOD16 products. Geographical Research, 32(4): 617-627. (in Chinese with English abstract)

Wu, G.P., Liu, Y.B., 2015a. Capturing variations in inundation with satellite remote sensing in a morphologically complex, large lake. Journal of Hydrology, 523(6): 14-23. DOI: 10.1016/j.jhydrol.2015.01.048.

Wu, G.P., Liu, Y.B., 2015b. Combining multispectral imagery with in situ Topographic data reveals complex water level variation in China's largest freshwater lake. Remote Sensing, 7(10): 13466-13484. DOI: 10.3390/rs71013466.

Ye, X., Zhang, Q., Liu, J., Li, X., Xu, C.Y., 2013. Distinguishing the relative impacts of climate change and human activities on variation of streamflow in the Poyang Lake catchment, China. Journal of Hydrology, 494(12): 83-95. DOI:

10.1016/j.jhydrol.2013.04.036.

Zedler, J.B., Kercher, S., 2005. Wetland resources: Status, trends, ecosystem services and restorability. Annual Review of Environment and Resources, 30: 39-74. DOI: 10.1146/annurev.energy.30.050504.144248.

Zhang, Q., Li, L., Wang, Y.-G., Werner, A.D., Xin, P., Jiang, T., Barry, D.A., 2012. Has the Three Gorges Dam made the Poyang Lake wetlands wetter and drier? Geophysical Research Letters, 39(20): L20402. DOI: 10.1029/2012GL053431.

Zhang, Q., Werner, A.D., 2015. Hysteretic relationships in inundation dynamics for a large lake–floodplain system. Journal of Hydrology, 527(4): 160-171. DOI: 10.1016/j.jhydrol.2015.04.068.

Zhang, Q., Werner, A.D., Aviyanto, R.F., Hutson, J.L., 2009. Influence of soil moisture hysteresis on the functioning of capillary barriers. Hydrological Processes, 23(9): 1369–1375. DOI: 10.1002/hyp.7261.

Zhang, Q., Ye, X., Werner, A.D., Li, Y., Yao, J., Li, X., Xu, C., 2014. An investigation of enhanced recessions in Poyang Lake: Comparison of Yangtze River and local catchment impacts. Journal of Hydrology, 517: 425-434. DOI: 10.1016/j.jhydrol.2014.05.051.

Table 1. Data of selected remotely sensed imagery, corresponding stage measured at Duchang Station and deciphered water surface area, which are ordered by the

stage.

Data	Stage (m)	Water surface area (km^2)
12 Feb 2009	8.15	561
14 Jan 2010	8.42	683
26 Oct 2009	8.87	547
15 Feb 2004	9.07	533
15 Dec 2004	9.49	685
21 Dec 2006	9.96	808
10 Dec 2008	10.21	815
8 Jan 2002	10.41	795
21 Nov 2001	11.88	1239
27 Mar 2007	12.1	1375
5 Mar 2005	12.66	1611
19 Mar 2010	13.06	2035
20 Oct 2001	13.44	1571
10 Oct 2003	14.88	2216
29 Nov 2005	15.02	2186
21 May 2004	15.52	2380
12 Jun 2006	16.4	2664
2 Aug 2007	17.73	2634
4 Aug 2002	17.77	2937

Table 2. Degree of stage-flow hysteresis (ηQH) for each river (and total catchment inflow) and lake station

	Ganjiang	Fuhe	Xinjiang	Raohe	Xiushui	Catchment	Yangtze River
Hukou	0.366	0.285	0.337	0.35	0.319	0.401	0.011
Xingzi	0.365	0.296	0.349	0.347	0.322	0.405	0.037
Duchang	0.353	0.299	0.346	0.338	0.318	0.396	0.075
Tangyin	0.351	0.311	0.357	0.349	0.307	0.401	0.107
Kangshan	0.334	0.336	0.401	0.364	0.338	0.409	0.157

Table 3. The span (days) of Phase 2 from stage-flow functions, as derived from the data shown in Figure 4

	Ganjiang	Fuhe	Xinjiang	Raohe	Xiushui	Catchment	Yangtze River
Hukou	37	38	38	29	75	38	1
Xingzi	26	27	27	18	64	27	10
Duchang	26	27	27	18	64	27	10
Tangyin	10	11	11	2	48	11	26
Kangshan	9	10	10	1	47	10	27

Table 4. Degree of stage-area hysteresis (ηSH) for each lake station using Eq. (10) applied to normalized area and stage datasets obtained by applying Eqs. (6) and (7). Values are derived from the data shown in Figure 6(b).

Stations	η_{SH}
Hukou	0.105
Xingzi	0.078
Duchang	0.051
Tangyin	0.03
Kangshan	0.062

Highlights:

1. Remotely sensed imagery verifies lake area results of hydrodynamic model.

2. Measured river flows added to the characterization of the lake's hysteretic behavior.

3. Stage-flow relationships reveal a three-phase hydrological regime.

4. The lake's hysteretic behavior is the summation of lake, river and floodplain.

5. The river effect is the major factor causing the lake's hydrological functions.